Supporting Information

Evidence for Fast Lithium-Ion Diffusion and Charge-Transfer Reactions in Amorphous TiO_x Nanotubes: Insights for High-Rate Electrochemical Energy Storage

Yu Jiang, [*, a] *Charles Hall,*[a] *Ning Song,*[a] *Derwin Lau,*[a] *Patrick A Burr,*[b] *Robert Patterson,*[a] *Da-Wei Wang,*[c] *Zi Ouyang,*[a] *and Alison Lennon*[*, a]

[a] School of Photovoltaic and Renewable Energy Engineering, [b] School of Electrical Engineering and Telecommunication, UNSW Sydney, [c] Particles and Catalysis Research Group, School of Chemical Engineering, UNSW Sydney, Sydney, NSW 2052, Australia

Corresponding Author

*E-mail: yu.jiang1@unsw.edu.au (Y.J.)

*E-mail: a.lennon@unsw.edu.au (A.L.)

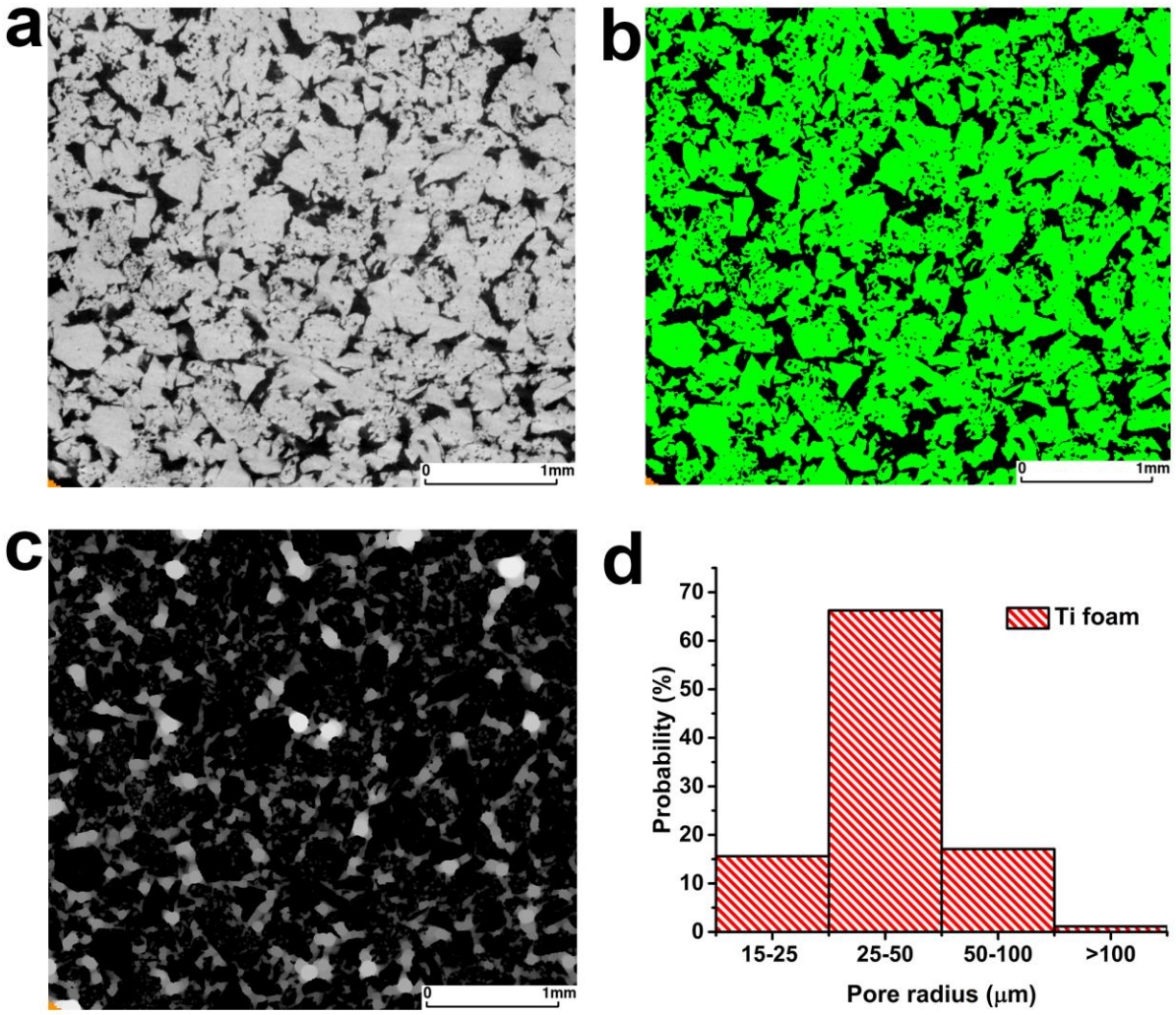

Figure S1. X-ray computed tomography analysis of the Ti foam. a) A reconstructed 3D tomogram with dark regions representing low-density materials (i.e., pore space) and bright regions signifying higher-density materials (Ti metal). b) A segmented tomogram with green and black colored regions representing Ti metal and pore space respectively. c) A covering radius transform (CRT) image with grey color scale proportional to the sphere radius. d) Pore size distribution estimated by CRT method.

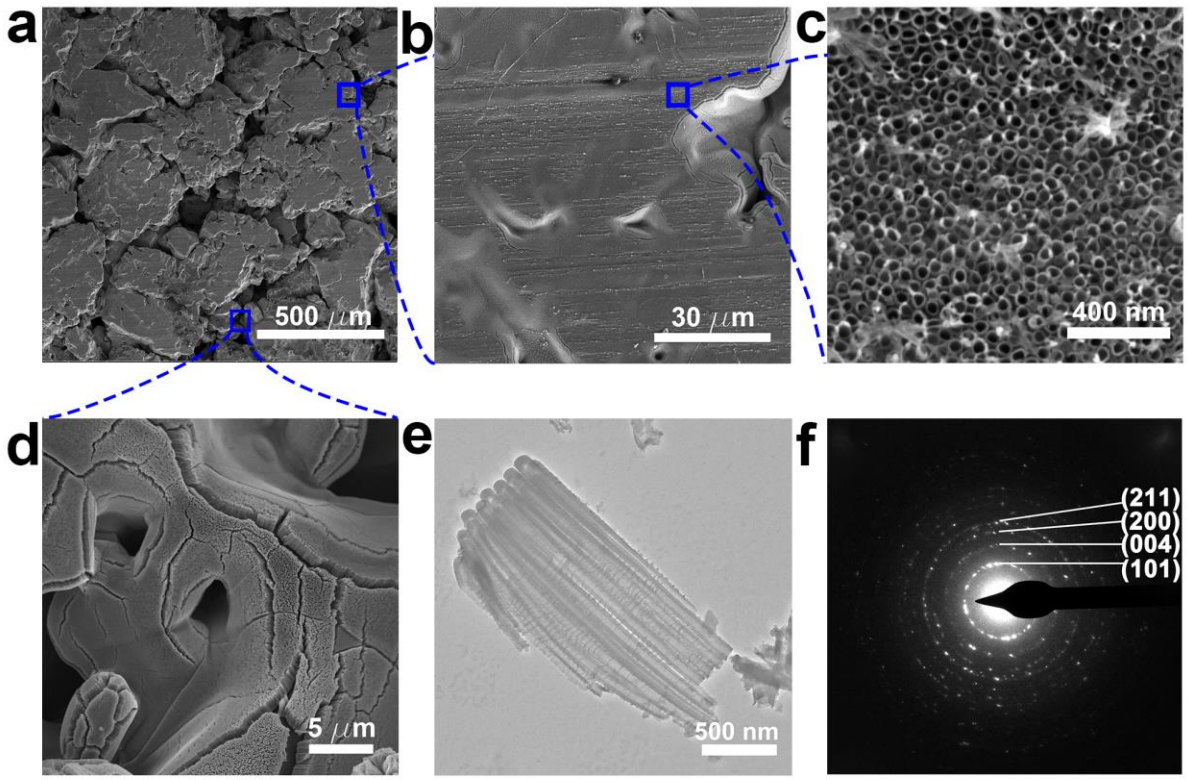

Figure S2. SEM images of a section of Ti foam after anodization in a) lower and b) higher magnifications. SEM image showing self-supported TiO_x NTs on the c) outer and d) inner surface of the Ti foam. e) TEM image of a-TiO_x NTs. f) SAED of c-TiO_x NTs with the first four diffraction rings being indexed to corresponding crystal planes of anatase TiO_2 ($I4_1/amd$).

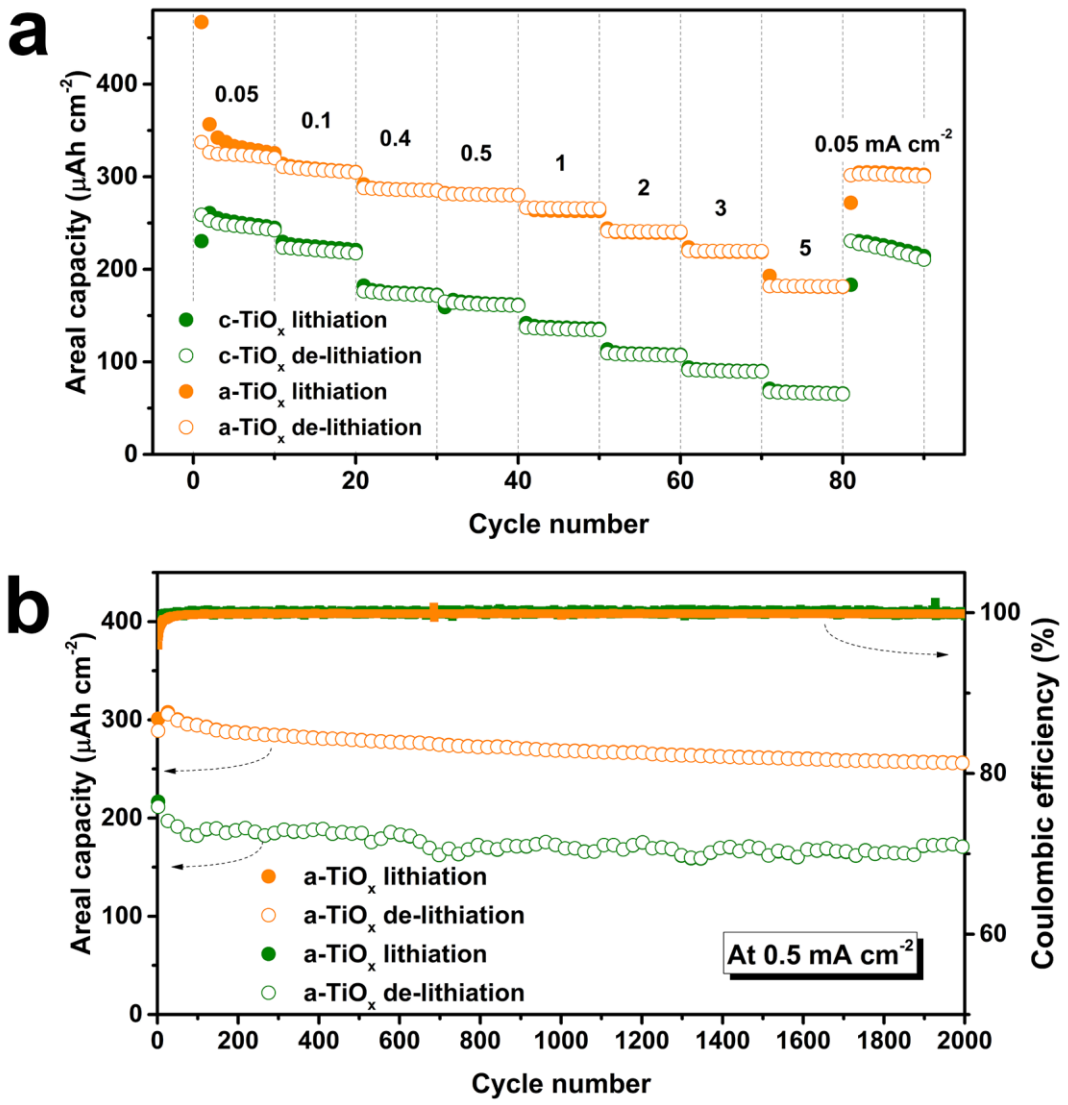

Figure S3. Per-area electrochemical performance of the a-TiO_x and c-TiO_x electrodes. Rate capability a), cycling stability and coulombic efficiencies b) of the a-TiO_x and c-TiO_x electrodes.

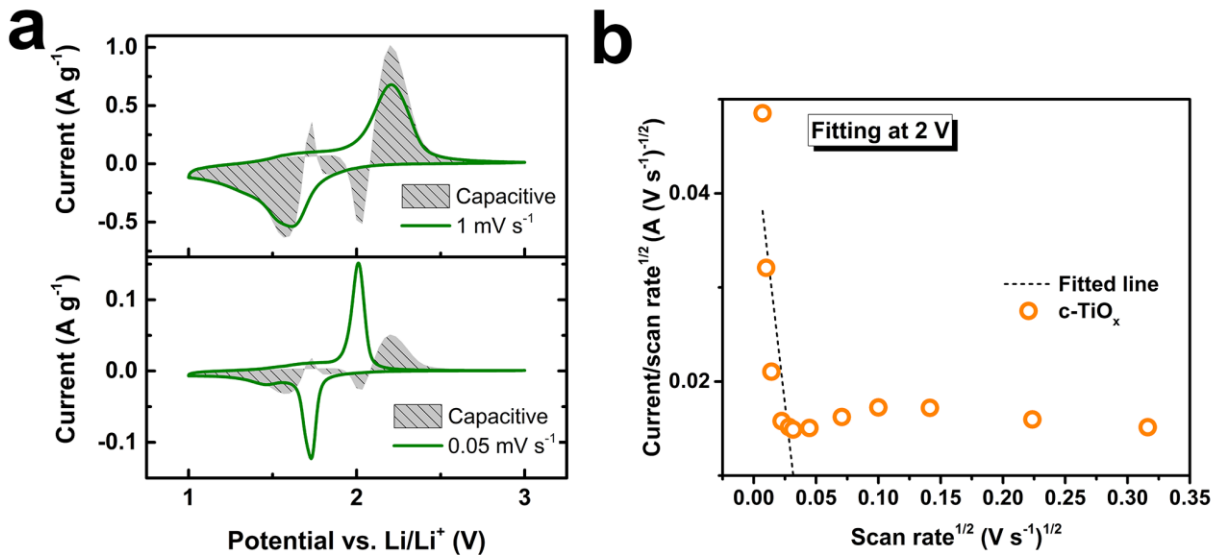

Figure S4. Charge storage mechanism analysis of the c-TiO_x electrode. a) Separation of the capacitive and diffusion current in the c-TiO_x electrode at scan rates of 0.05 (bottom) and 1 mV s^{-1} (top), respectively. b) Example determination of capacitive and diffusion relative contributions from the slope and intercept of fitted line for the c-TiO_x electrode at a potential of 2 V.

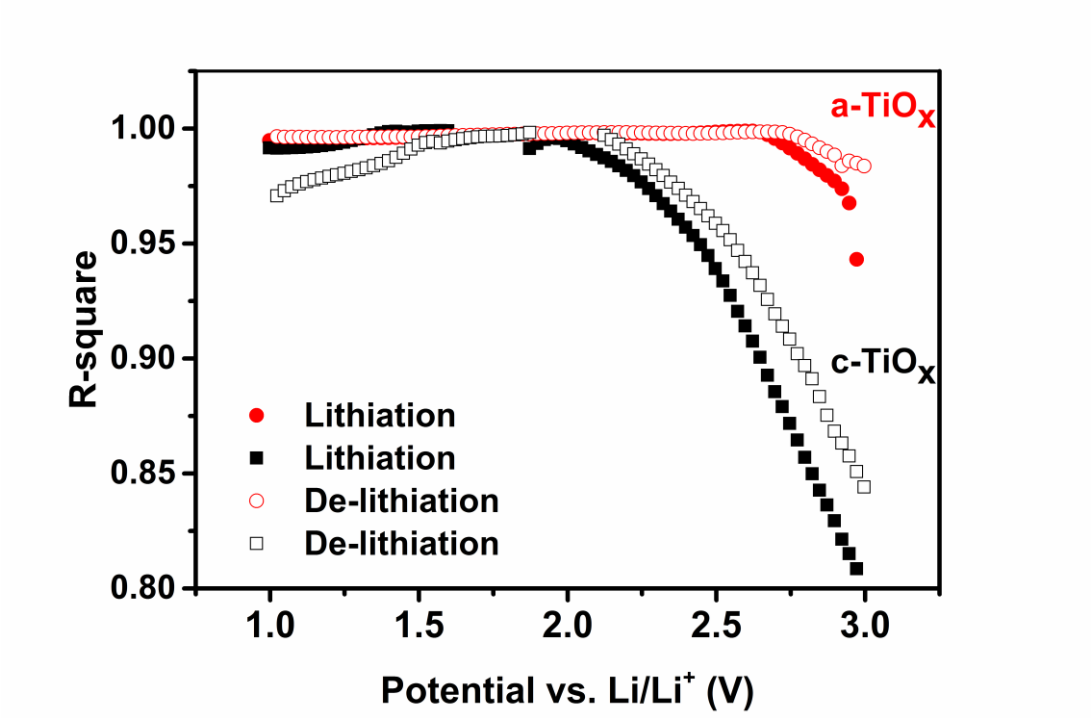

Figure S5. Coefficients of determination (*R*-square values) showing the goodness of fitting to the measured PITT data using the mixed-controlled insertion model for the a-TiO_x and c-TiO_x electrodes.

The goodness of fit using Montella's mixed-controlled insertion model was evaluated using an *R*-square analysis and *R*-square values >0.99 were attained by the fitting of a-TiO_x current transients at most potentials. The fit for the c-TiO_x electrode in overall represented the measured data less accurately. The calculated *R*-square values for the c-TiO_x electrode were comparable to the a-TiO_x electrode at potentials <2.25 V; however lower values (0.8-0.97) were obtained at potentials >2.25 V. In this potential range, the storage capacity of Li^+ in c-TiO_x due to charge-transfer reactions is relatively small resulting in the current responses to potential steps in this potential range being more affected by the EDL current and less accurately described by the Montella's model. Additionally, fitting inaccuracy may also arise from the data acquisition

instrument which was limited by its accuracy in measuring the very low current values in the long-time domain.

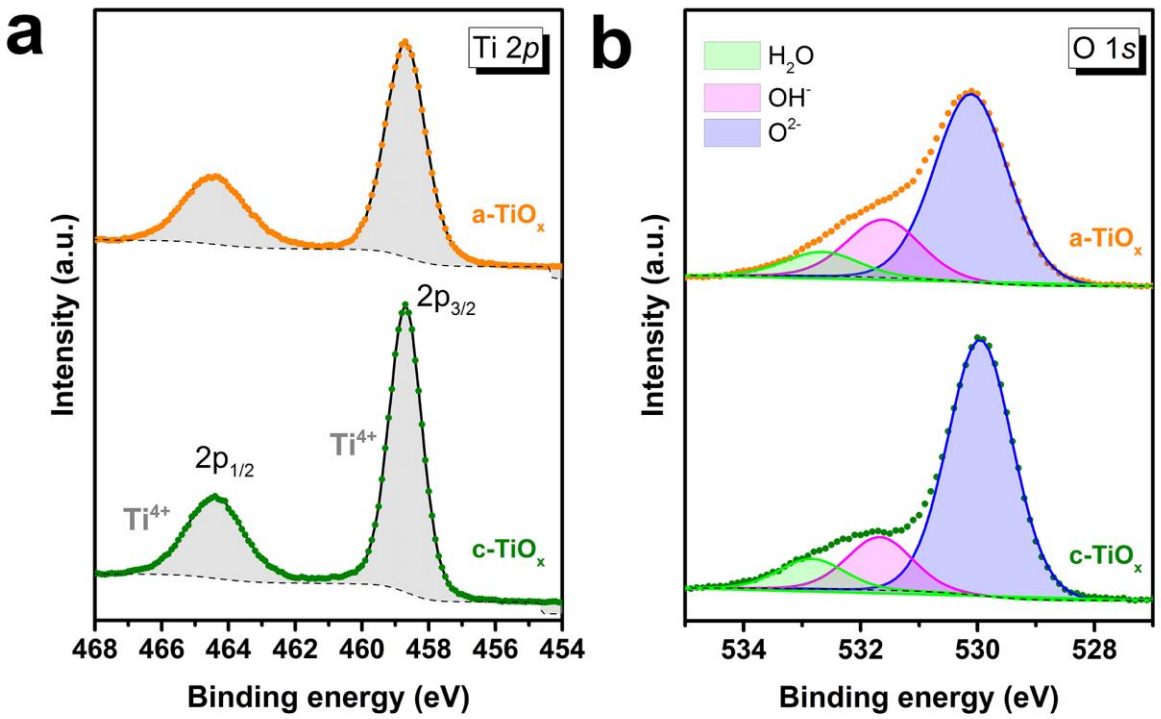

Figure S6. a) Ti 2p core-level XPS spectra and b) O 1s core-level XPS spectra of the a-TiO_x and c-TiO_x NT electrodes.

Figure S6b compares the O 1s core-level spectra between the a-TiO_x and c-TiO_x electrodes. Both electrodes exhibited a main peak at ~ 529.9 eV, corresponding to the characteristic peak of lattice oxygen in TiO_2.[1] Additional two peaks at ~ 531.6 eV and ~ 532.7 eV were evident in the spectra of both electrodes, which have been observed previously for TiO_2 films in the literature and were attributed respectively to bridging hydroxyls (Ti-OH) and physisorbed molecular water (H_2O) on TiO_2 surface.[2-3] A considerable content of physisorbed water was found on the surface of both electrodes possibly due to the electrodes being exposed to the air ambient before the XPS measurement. The Ti-OH peak density of a-TiO_x was relatively higher than that of c-TiO_x, indicating the amount of hydroxyl groups on the a-TiO_x surface was reduced after thermal annealing at 400 °C.

Table S1. Comparison of per-weight electrochemical performance between the a-TiO_x/Ti foam electrode in this study and other TiO_x NT electrodes in the literature. The 1 C value was defined as 168 mA g^{-1} corresponding to 1 hour charge/discharge current of a theoretical capacity of 168 mAh g^{-1} which assumes a stoichiometry of 0.5 Li per TiO_2 formula unit.

Electrodes	Tube length (μm)	Wall thickness (nm)	Capacity (mAh g^{-1})		Cycling lifetime	Capacity retention	Ref.
			low rate	high rate			
a-TiO_x/ Ti foam	**2.4**	**30**	**135 (0.125 C)**	**77 (12.5 C)**	**2000**	**92%**	**This work**
c-TiO_x/ Ti foam	**2.3**	**30**	**102 (0.125 C)**	**28 (12.5 C)**	**2000**	**80%**	**This work**
a-TiO_x/ Ti foil	1.0	/	229 (6 C)	123 (298 C)	100	~ 96%	[4]
a-TiO_x/ Ti foil	0.35	17	230 (0.3 C)	/	200	78%	[5]
a-TiO_x/ Ti foil	6.0	15	275 (1.2 C)	80 (96 C)	2100	50%	[6]
a-TiO_x/ Ti foil	0.2 – 7.8	/	180 (0.25 C)	130 (5 C)	30	/	[7]
a-TiO_x/ Ti foil	/	/	271 (0.3 C)	135 (101 C)	600	~ 95%	[8]
c-TiO_x/ Ti foil	1.0	/	108 (6 C)	30 (89 C)	100	/	[4]
c-TiO_x/ Ti foil	1.7	12	190 (0.25 C)	50 (5C)	/	/	[9]
c-TiO_x/ Ti foil	/	/	165-210 (0.15 C)	30 (3 C)	50	76%	[10]
c-TiO_x/ Ti disc	1.5	10	172 (0.05 C)	38 (50 C)	320	/	[11]

Table S2. Comparison of per-area electrochemical performance between the a-TiO_x/Ti foam electrode in this study and other TiO_x NT electrodes in the literature.

Electrodes	Tube length (μm)	Wall thickness (nm)	Capacity (μAh cm^{-2})		Cycling lifetime	Capacity retention	Ref.
			low rate	high rate			
a-TiO_x/ Ti foam	**2.4**	**30**	**324 (50 μA cm^{-2})**	**182 (5 mA cm^{-2})**	**2000**	**92%**	**This work**
c-TiO_x/ Ti foam	**2.3**	**30**	**246 (50 μA cm^{-2})**	**66 (5 mA cm^{-2})**	**2000**	**80%**	**This work**
a-TiO_x/ Ti foam	1.5	/	103 (10 μA cm^{-2})	83 (0.5 mA cm^{-2})	100	100%	[12]
a-TiO_x/ Ti foil	0.92	20	77 (5 μA cm^{-2})	44 (0.1 mA cm^{-2})	50	71%	[13]
a-TiO_x/ Ti disc	> 15 μm	16	815-200 (1st - 450th cycle) (0.5 mA cm^{-2})		450	25%	[14]
c-TiO_x/ Ti foil	0.92	20	68 (5 μA cm^{-2})	30 (0.1 mA cm^{-2})	50	71%	[13]
c-TiO_x/ Ti disc	26	/	200 (10 μA cm^{-2})	115 (0.4 mA cm^{-2})	100	88%	[15]

Table S3. Fitted parameters for the EIS equivalent circuit model.

Electrodes	R_Ω ohm	R_{ct} ohm	CPE Q F $s^{\alpha-1}$	CPE α	Z_w R_d ohm	Z_w τ_d s	C_{int} F	D $cm^2\ s^{-1}$
a-TiO_x	7	29	1.1×10^{-4}	0.747	146	108	1.02	2.1×10^{-14}
c-TiO_x	5	78	4.0×10^{-5}	0.798	6641	7847	0.14	2.9×10^{-16}

REFERENCES

(1) Lu, X.; Wang, G.; Zhai, T.; Yu, M.; Gan, J.; Tong, Y.; Li, Y. Hydrogenated TiO_2 Nanotube Arrays for Supercapacitors. *Nano Lett.* **2012,** *12* (3), 1690-1696.

(2) Ketteler, G.; Yamamoto, S.; Bluhm, H.; Andersson, K.; Starr, D. E.; Ogletree, D. F.; Ogasawara, H.; Nilsson, A.; Salmeron, M. The Nature of Water Nucleation Sites on TiO_2(110) Surfaces Revealed by Ambient Pressure X-Ray Photoelectron Spectroscopy. *J. Phys. Chem. C* **2007,** *111* (23), 8278-8282.

(3) Li, L.; Yan, J.; Wang, T.; Zhao, Z.-J.; Zhang, J.; Gong, J.; Guan, N. Sub-10 nm Rutile Titanium Dioxide Nanoparticles for Efficient Visible-Light-Driven Photocatalytic Hydrogen Production. *Nat. Commun.* **2015,** *6*, 5881.

(4) Fang, H. T.; Liu, M.; Wang, D. W.; Sun, T.; Guan, D. S.; Li, F.; Zhou, J.; Sham, T. K.; Cheng, H. M. Comparison of the Rate Capability of Nanostructured Amorphous and Anatase TiO_2 for Lithium Insertion Using Anodic TiO_2 Nanotube Arrays. *Nanotechnology* **2009,** *20* (22), 225701.

(5) Wu, Q. L.; Li, J.; Deshpande, R. D.; Subramanian, N.; Rankin, S. E.; Yang, F.; Cheng, Y.-T. Aligned TiO_2 Nanotube Arrays as Durable Lithium-Ion Battery Negative Electrodes. *J. Phys. Chem. C* **2012,** *116* (35), 18669-18677.

(6) Lamberti, A.; Garino, N.; Sacco, A.; Bianco, S.; Chiodoni, A.; Gerbaldi, C. As-Grown Vertically Aligned Amorphous TiO_2 Nanotube Arrays as High-Rate Li-Based Micro-Battery Anodes with Improved Long-Term Performance. *Electrochim. Acta* **2015,** *151*, 222-229.

(7) Anwar, T.; Wang, L.; Tongxiang, L.; He, X.; Sagar, R. U. R.; Shehzad, K. Effect of Aspect Ratio of Titanium Dioxide Nanotube Arrays on the Performance of Lithium Ion Battery. *Int J Electrochem Sci* **2015,** *10* (7), 6537-6547.

(8) Xiong, H.; Yildirim, H.; Shevchenko, E. V.; Prakapenka, V. B.; Koo, B.; Slater, M. D.; Balasubramanian, M.; Sankaranarayanan, S. K. R. S.; Greeley, J. P.; Tepavcevic, S.; Dimitrijevic, N. M.; Podsiadlo, P.; Johnson, C. S.; Rajh, T. Self-Improving Anode for Lithium-Ion Batteries Based on Amorphous to Cubic Phase Transition in TiO_2 Nanotubes. *J. Phys. Chem. C* **2012,** *116* (4), 3181-3187.

(9) Zhu, K.; Wang, Q.; Kim, J.-H.; Pesaran, A. A.; Frank, A. J. Pseudocapacitive Lithium-Ion Storage in Oriented Anatase TiO_2 Nanotube Arrays. *J. Phys. Chem. C* **2012,** *116* (22), 11895-11899.

(10) Wang, Y.; Liu, S.; Huang, K.; Fang, D.; Zhuang, S. Electrochemical Properties of Freestanding TiO_2 Nanotube Membranes Annealed in Ar for Lithium Anode Material. *J. Solid State Electrochem.* **2012,** *16* (2), 723-729.

(11) Auer, A.; Portenkirchner, E.; Götsch, T.; Valero-Vidal, C.; Penner, S.; Kunze-Liebhäuser, J. Preferentially Oriented TiO_2 Nanotubes as Anode Material for Li-Ion Batteries: Insight into Li-Ion Storage and Lithiation Kinetics. *ACS Appl. Mater. Interfaces* **2017,** *9* (42), 36828-36836.

(12) Bi, Z.; Paranthaman, M. P.; Menchhofer, P. A.; Dehoff, R. R.; Bridges, C. A.; Chi, M.; Guo, B.; Sun, X.-G.; Dai, S. Self-Organized Amorphous TiO_2 Nanotube Arrays on Porous Ti Foam for Rechargeable Lithium and Sodium Ion Batteries. *J. Power Sources* **2013,** *222* (Supplement C), 461-466.

(13) Ortiz, G. F.; Hanzu, I.; Djenizian, T.; Lavela, P.; Tirado, J. L.; Knauth, P. Alternative Li-Ion Battery Electrode Based on Self-Organized Titania Nanotubes. *Chem. Mater.* **2009,** *21* (1), 63-67.

(14) Madian, M.; Klose, M.; Jaumann, T.; Gebert, A.; Oswald, S.; Ismail, N.; Eychmuller, A.; Eckert, J.; Giebeler, L. Anodically Fabricated TiO_2-SnO_2 Nanotubes and Their Application in Lithium Ion Batteries. *J. Mater. Chem. A* **2016,** *4* (15), 5542-5552.
(15) Madian, M.; Giebeler, L.; Klose, M.; Jaumann, T.; Uhlemann, M.; Gebert, A.; Oswald, S.; Ismail, N.; Eychmüller, A.; Eckert, J. Self-Organized TiO_2/CoO Nanotubes as Potential Anode Materials for Lithium Ion Batteries. *ACS Sustainable Chem. Eng.* **2015,** *3* (5), 909-919.